Annals of Nuclear Energy
Manuscript Draft

Manuscript Number: ANUCENE-D-18-00096

Title: Code Validation of a Scaled-down DRACS Model in RELAP5/SCDAPSIM/MOD 4.0

Article Type: VSI: Advancing FHR technology

Keywords: RELAP5; DRACS; FHR; AHTR; Code validation; Natural circulation

Abstract:
Direct Reactor Auxiliary Cooling System (DRACS) is a passive safety system proposed for Fluoride-salt-cooled High-temperature Reactors (FHRs). Benchmark study of decay heat removal capability of DRACS by natural circulation is critical for FHR safety analysis. Two scaled-down test facilities, a low-temperature DRACS test facility (LTDF) and a high-temperature DRACS test facility (HTDF), were designed following a scaling analysis and constructed to investigate thermal performance and heat removal capability of the DRACS. The LTDF uses water as a surrogate coolant for both the primary and DRACS loops. Two transient scenarios were carried out in the LTDF, namely, DRACS startup and primary coolant pump trip. In both of the scenarios, the experimental results demonstrate sufficient heat 2

removal capabilities of the DRACS with natural circulations established in the system. These two scenarios were simulated using RELAP5 SCDAPSIM/MOD 4.0 code and the code simulation results show good agreement with the LTDF experimental data. For the HTDF, molten salts FLiNaK and KF-ZrF4 are used respectively as the primary coolant and DRACS coolant. Thermodynamic and transport properties of FLiNaK and KF-ZrF4 were implemented into RELAP5/SCDAPSIM/MOD 4.0. Simulations of transient scenarios in the HTDF were also performed and the code results will be compared with the HTDF experimental data once available.

*Manuscript
Click here to view linked References

Code Validation of a Scaled-down DRACS Model in RELAP5/SCDAPSIM/MOD 4.0

Hsun-Chia Lin[a, b], Qiuping Lv[a, c], Shanbin Shi[a, b], Xiaodong Sun[a, b], Richard Christensen[a,d], Graydon Yoder[e]

[a] *Nuclear Engineering Program, Department of Mechanical and Aerospace Engineering, The Ohio State University, 201 W 19th Avenue, Columbus, OH 43210, USA*

[b] *Department of Nuclear Engineering and Radiological Sciences, University of Michigan, 2355 Bonisteel Blvd, Ann Arbor, MI, 48109, USA*

[c] *Argonne National Laboratory, 9700 Cass Ave, Lemont, IL 60439, USA*

[d] *Department of Nuclear Engineering, University of Idaho,1776 Science Center Drive, Idaho Falls, ID 83402 USA*

[e] *Oak Ridge National Laboratory, Oak Ridge, TN 37831, USA*

Abstract

Direct Reactor Auxiliary Cooling System (DRACS) is a passive safety system proposed for Fluoride-salt-cooled High-temperature Reactors (FHRs). Benchmark study of decay heat removal capability of DRACS by natural circulation is critical for FHR safety analysis. Two scaled-down test facilities, a low-temperature DRACS test facility (LTDF) and a high-temperature DRACS test facility (HTDF), were designed following a scaling analysis and constructed to investigate thermal performance and heat removal capability of the DRACS. The LTDF uses water as a surrogate coolant for both the primary and DRACS loops. Two transient scenarios were carried out in the LTDF, namely, DRACS startup and primary coolant pump trip. In both of the scenarios, the experimental results demonstrate sufficient heat

removal capabilities of the DRACS with natural circulations established in the system. These two scenarios were simulated using RELAP5 SCDAPSIM/MOD 4.0 code and the code simulation results show good agreement with the LTDF experimental data. For the HTDF, molten salts FLiNaK and KF-ZrF_4 are used respectively as the primary coolant and DRACS coolant. Thermodynamic and transport properties of FLiNaK and KF-ZrF_4 were implemented into RELAP5/SCDAPSIM/MOD 4.0. Simulations of transient scenarios in the HTDF were also performed and the code results will be compared with the HTDF experimental data once available.

1. Introduction

Fluoride-salt-cooled High-temperature Reactor (FHR) is one of the advanced reactors that combines improved technologies including low-pressure fluoride salt coolant, coated tristructural-isotropic (TRISO) particle fuel, Brayton power cycle, and passive safety systems. These features provide advantages including increased thermal efficiency, low operation pressure, high core power density, and high safety characteristics (Forsberg, 2005; Bardet et al., 2008). One of the major safety systems proposed for FHRs, Direct Reactor Auxiliary Cooling System (DRACS), is capable of removing decay heat passively. The DRACS was originally developed for Experimental Breeder Reactor II (EBR-II) (Roglans et al., 1993) and has been widely adopted in pool-type reactors, e.g., Sodium Fast Reactors (SFRs) and FHRs (Zhang et al., 2009; Forsberg et al., 2003). In the DRACS, three natural circulation/convection loops are coupled through two heat exchangers, namely, the DRACS Heat Exchanger (DHX) and Natural Draft Heat Exchanger (NDHX), which enable decay heat removal from the reactor core to the ambient air. The performance of decay heat removal in such a system is significantly affected by the designs of both the DHX and NDHX. Fluidic diode that is utilized as a passive flow controller is another key component in the DRACS. The functionality of the fluidic diode

limits parasitic heat loss into the DRACS during reactor normal operation, while it ensures a sufficient decay heat removal capability when the reactor is shutdown during accidents.

To support the FHR development and licensing, it is critical to investigate, both experimentally and numerically, the DRACS thermal performance and scalability for developing an optimum DRACS design and ensuring reactor safety under accident conditions (Holcomb et al., 2009). The primary objective of this study is to perform a code validation of RELAP5/SCDAPSIM/MOD 4.0 on the DRACS thermal performance and to analyze the establishment of natural circulation flows in the DRACS. Based on a prototypic DRACS design for a 20-MWth test FHR, two scaled-down DRACS test facilities were designed following a detailed scaling analysis to study the thermal performance of the DRACS, including the natural circulation/convection flow during transients, and heat exchanger testing for FHR applications (Lv et al., 2015; Chen et al., 2015; Chen et al., 2016). A low-temperature DRACS test facility (LTDF) that uses water as a surrogate to molten salts and a high-temperature DRACS test facility (HTDF) that uses molten salts, namely, FLiNak and KF-ZrF_4, as the primary and intermediate coolant salts, were constructed at The Ohio State University (OSU). An extensive test matrix was developed for the LTDF and experiments were carried out accordingly. The experimental results confirmed the establishment of natural circulation flows and sufficient capability of removing the decay heat in the LTDF (Lv et al., 2016). In addition, a MATLAB computer code was developed for analyzing the thermal performance of the HTDF. The simulation results by the MATLAB code showed good agreement with the HTDF design values (Lv et al., 2015).

To perform numerical analyses for FHRs using a system-level analysis code, Davis et al. (2005) implemented the thermophysical properties of four molten salts, namely, FLiBe, FLiNaK,

$NaBF_4$-NaF, and NaF-ZrF_4, into the RELAP5-3D/ATHENA code. The implemented salt properties, including the salt thermodynamic and transport properties as a function of temperature were obtained from Williams et al. (2006). Two more molten salts, KF-ZrF_4 and KCL-$MgCl_2$, were also studied by Anderson et al. (2012) for system code implementation. In this study, we have selected RELAP5/SCDAPSIM/MOD 4.0 (Allison et al., 2016) as the system-level analysis tool to develop accurate numerical models for both the LTDF and HTDF. Both RELAP5 DRACS models include heat loss calculation and heat transfer correlation implementation for the DHX and NDHX, and molten salt property implementation for the HTDF.

2. Experimental Facilities

2.1. Low-Temperature DRACS Facility

The LTDF was built, following a detailed scaling study, to investigate the decay heat removal performance by natural circulation (Figure 1 and 2) (Lv et al., 2015; Lv et al., 2016). Pressurized (10 bar) distilled water is used as a surrogate to molten salt in the primary loop and distilled water near the atmospheric pressure is used as the working fluid in the DRACS loop (i.e., the "secondary" loop in the LTDF). Three electric cartridge heaters, each rated at 2 kW, are used to simulate the core heating in the primary loop. These 1.0-m long heater rods with stainless steel 304 (SS304) sheath are vertically oriented and arranged in a triangular pattern. The water in the primary loop is pressurized to eliminate any potential of water boiling on the heater rod sheath surface. A primary pump is installed in the primary loop to drive the flow prior to a transient that would lead to the shutdown of the reactor and the initiation of the natural circulation flow in the primary loop. In addition, a fluid diode simulator is used in the LTDF, in which two ball valves provide two distinctively different flow resistances in the two opposite

flow directions (i.e., very large flow resistance in the upward flow direction but significantly smaller flow resistance in the downward direction). Two heat exchangers in the LTDF, namely, the DHX and NDHX, transfer heat from the primary coolant, i.e., pressurized water to the ambient air. Their design parameters are summarized in Table 1 (Lv et al., 2015).

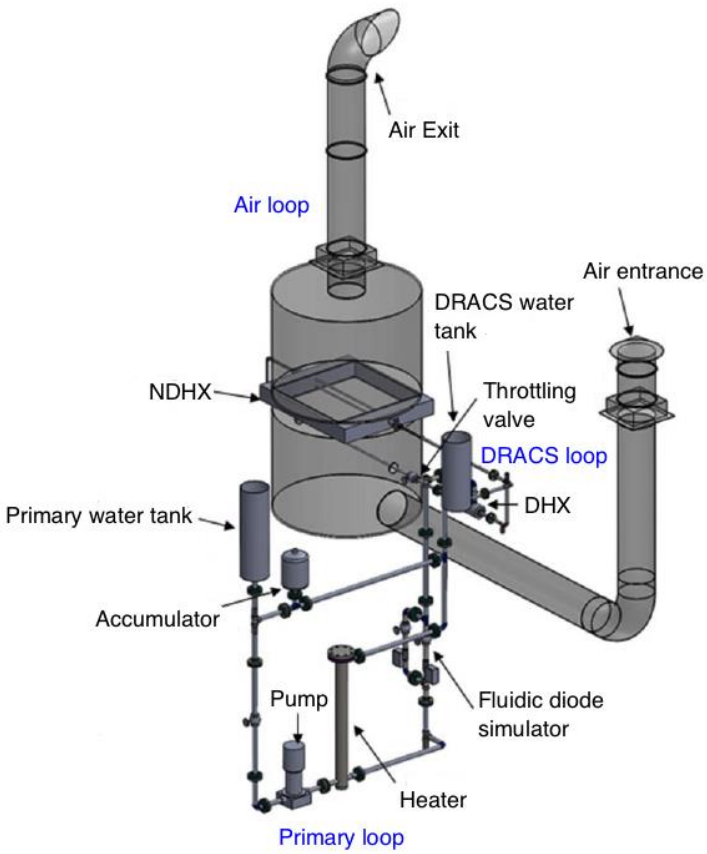

Figure 1. Three-dimensional layout of the LTDF (Lv et al., 2015).

Figure 2. A photograph of the LTDF (Lv et al., 2015).

Table 1. Design parameters of the DHX and NDHX in the LTDF (Lv et al., 2015).

Item	Specification	Value
DHX	Heat exchanger type	Shell-and-tube
	Tube outer diameter (inch)	0.375
	Tube thickness (inch)	0.044
	Tube Number	80
	Pitch to diameter ratio	1.208
	Tube length (in)	14
	Shell inner diameter (inch)	5
	Baffles number and baffle cut	4 and 25.8%
	Material	SS316
NDHX	Heat exchanger type	Finned tube bundle
	Tube outer diameter (inch)	0.625
	Tube thickness (inch)	0.035
	Tube Number	52 (in 2 rows)
	Pitch to diameter ratio	2.4
	Tube length (inch)	39
	Fin height (inch)	0.475
	Fin thickness (inch)	0.01
	Fin spacing (inch)	0.1
	Material	Copper tube + Aluminum fin

In the LTDF, T-type thermocouples, ultrasonic flow meters, and a thermal mass flow meter are used to measure the fluid temperatures, water flow rates (for both the primary and DRACS loops), and air flow rate, respectively. The measurement uncertainties (including both the

systematic uncertainties associated with the instruments and the random uncertainties associated with the measured data) of the fluid temperatures, water and air flow rates are estimated as ±0.5 ºC, ±20%, and ±10% respectively, with a 95% confidence level (Lv et al., 2016).

2.2. High-Temperature DRACS Facility

The overall structure of the HTDF is similar to the LTDF, but the coolants in the primary and DRACS loops are FLiNaK and KF-ZrF_4, respectively. Seven electric cartridge heaters are used in the simulated core, with a total nominal power of 10 kW (The total actual heating capacity of the seven heaters is 70 kW). A disc-shape vortex diode is employed as a passive flow controller in the primary loop (Lv et al., 2013). The shell-and-tube type DHX is vertically oriented and consists of a total of 80 5/8'' BWG-18 tubes, each with a length of 0.325 m. For the NDHX in the HTDF, 36 plain tubes (1/2'' BWG-16) are arranged in a staggered fashion in two rows (Lv et al., 2014). The entire HTDF facility is made of stainless steel 316H.

3. RELAP5 Modeling

3.1. LTDF and HTDF Models

One-dimensional LTDF and HTDF models have been built and developed in the RELAP5/SCDAPSIM/MOD 4.0 code and their nodalization is shown in Figure 3. In the air loop, a time-dependent volume is utilized to simulate the source of the ambient air. During the 10-hour LTDF test, the air inlet temperature decreases gradually from the day time to night. The decreasing inlet air temperature is therefore defined in the time-dependent volume as one of the boundary conditions for the LTDF. Both the LTDF and the HTDF contain four sets of heat structures, including the simulated core, DHX, NDHX, and pipe covered with thermal

insulation. The mesh numbers for the heater, DHX, and NDHX are 25, 50, and 50, respectively. Table 2 shows the heat transfer correlations utilized to model the heat transfer on the DHX shell side and NDHX air side. These correlations have been implemented into the RELAP5/SCDAPSIM/MOD 4.0 code. Prandtl number specified on the bulk fluid temperature and wall temperature are assumed the same in the implemented correlations.

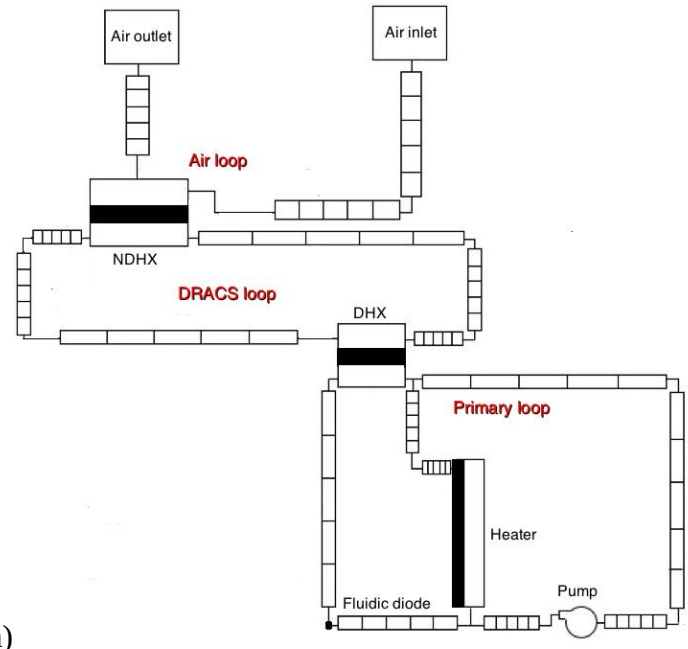

(a)

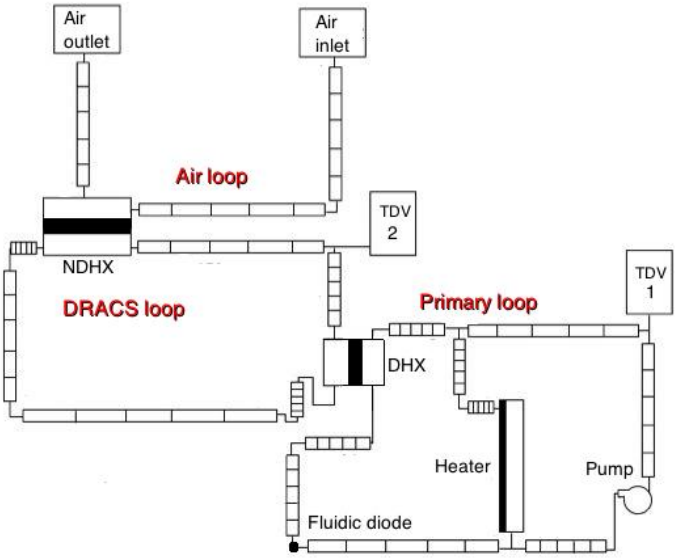

(b)

Figure 3. (a) LTDF and (b) HTDF models in RELAP5.

Table 2. Implemented heat transfer correlations for the DHX shell side and NDHX finned tube side

Item	Implemented correlations	Applicability	
DHX shell side (Žkauskas,1987)	$Nu = 1.04Re^{0.4}Pr^{0.36}(Pr/Pr_w)^{0.25}$	$1 \leq Re < 500$	(1)
	$Nu = 0.71Re^{0.5}Pr^{0.36}(Pr/Pr_w)^{0.25}$	$500 \leq Re < 1{,}000$	(2)
	$Nu = 0.35Re^{0.6}Pr^{0.36}\left(\frac{X_t^*}{X_l^*}\right)^{0.2}(Pr/Pr_w)^{0.25}$	$1{,}000 \leq Re < 2 \times 10^5$	(3)
	$Nu = 0.031Re^{0.8}Pr^{0.36}\left(\frac{X_t^*}{X_l^*}\right)^{0.2}(Pr/Pr_w)^{0.25}$	$Re \geq 2 \times 10^5$	(4)
NDHX finned tube side (Zukauskas and Ulinskas, 1988)	$Nu = 0.192Re^{0.65}Pr^{0.36}\left(\frac{X_t^*}{X_l^*}\right)^{0.2}\left(\frac{s}{d_0}\right)^{0.18}\left(\frac{e_f}{d_0}\right)^{-0.14}$	$100 \leq Re < 2 \times 10^4$	(5)
	$Nu = 0.0507Re^{0.8}Pr^{0.36}\left(\frac{X_t^*}{X_l^*}\right)^{0.2}\left(\frac{s}{d_0}\right)^{0.18}\left(\frac{e_f}{d_0}\right)^{-0.14}$	$2 \times 10^4 \leq Re < 2 \times 10^5$	(6)
	$Nu = 0.0081Re^{0.95}Pr^{0.4}\left(\frac{X_t^*}{X_l^*}\right)^{0.2}\left(\frac{s}{d_0}\right)^{0.18}\left(\frac{e_f}{d_0}\right)^{-0.14}$	$2 \times 10^5 \leq Re$	(7)

Here, $X_t^*, X_l^*, Re, Pr, Pr_w, \mathrm{S}, e_f, d_o$ are the relative transverse tube spacing, relative longitudinal tube spacing, Reynolds number, Prandtl number based on the fluid properties specified at the fluid average temperature, Prandtl number based on the fluid properties specified at the wall temperature, fin spacing, fin height, and tube outer diameter, respectively.

In the version of the RELAP5/SCDAPSIM/MOD 4.0 code available to the authors, no molten salt properties were available since the code was primarily developed for light water reactor transient simulations. According to the literature, some correlations for molten salt thermophysical properties were developed for implementation into reactor system codes (Davis et al., 2005; Williams et al., 2006; Anderson et al., 2012). The properties of two molten salts, FLiNaK and KF-ZrF_4, were therefore implemented into our current RELAP5

SCDAPSIM/MOD 4.0 code version for our planned HTDF thermal performance analysis. Table 3 summarizes the fluid salt properties as a function of their temperatures (K).

Table 3. Molten salt properties of FLiNaK and KF-ZrF_4 (Davis et al., 2005; Williams et al., 2006; Anderson et al., 2012).

FLiNaK		Uncertainty
Density (kg/m^3)	$-0.73(\mathrm{T}-273.15)+2530$	±5%
Thermal expansion coefficient (1/K)	$0.73/[-0.73(\mathrm{T}-273.15)+2530]$	±5%
Dynamic viscosity (kg/m-s)	$4\times10^{-5}e^{4170/T}$	±10%
Surface tension (N/m)	$0.26-1.2\times10^{-4}(T-273.15)$	+30%; -10%
Thermal conductivity (W/m-K)	$5\times10^{-4}e^{4170/T}+0.4348$	-
Heat capacity (J/kg-K)	1,884	±5%
KF-ZrF_4		Uncertainty
Density (kg/m^3)	$-0.887(\mathrm{T}-273.15)+3416$	±5%
Thermal expansion coefficient (1/K)	$0.887/[-0.887(\mathrm{T}-273.15)+3416]$	±5%
Dynamic viscosity (kg/m-s)	$1.59\times10^{-5}e^{3179/T}$	±10%
Surface tension (N/m)	$0.182-7.134\times10^{-5}T$	±1.5%
Thermal conductivity (W/m-K)	$5\times10^{-4}e^{4170/T}-0.032$	-
Heat capacity (J/kg-K)	1,046	-

3.2. Heat Loss Model

For code benchmark analysis, heat losses from the experimental facilities during experiments should be carefully considered, especially for the small-scale and high-temperature equipment. A heat loss model calculates the heat deposit in the structure walls and heat transfer from the walls to the room environment. The model includes the pipe walls, structure walls, and flanges. These structures are wrapped around by a layer of 2-inch-thick fiberglass, as shown in Figure

4. In the surrounding, a convective boundary is given and the room temperature is set based on the experimental condition. Though the heat balance analysis was performed based on the experimental data, the large measurement uncertainties in the fluid flow rates make the heat loss challenging to be quantified (Lv et al. 2015). From the simulation results, the total heat loss in the LTDF is about 7% based on a total heating power of 2 kW provided in the core when the DRACS system reaches a steady state.

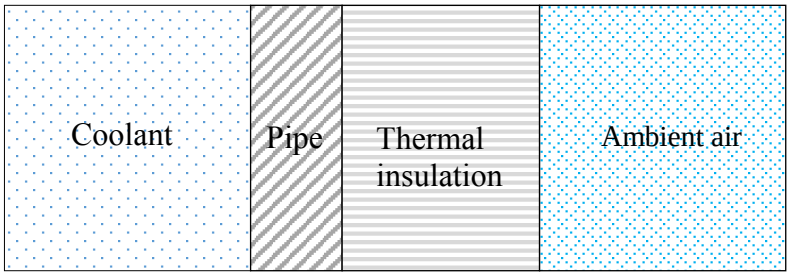

Figure 4. Wall structure and thermal insulation in the heat loss model.

In the HTDF, the issue of system heat losses to the environment is even more significant since the salt temperatures will be much higher than the water temperatures in the LTDF, up to 700 °C (or even higher under some accidental conditions). To reduce the heat losses in the HTDF, a layer of 5-inch thick microporous insulation was chosen due to its low thermal conductivity. The heat loss model shows that the total heat loss from the HTDF system is about 3% of the total 10-kW heating from the cartridge heaters. While the construction of the HTDF was completed at OSU, this research group recently joined the University of Michigan (UM) and therefore no experiments were performed in the HTDF yet. The HTDF has been transferred to UM and it is expected that some molten salt experimental data will be made available once the facility is re-assembled and operable at UM. The salt temperatures with the heat loss model implemented are about 10 °C lower when the system reaches a steady state as compared to

those without the heat loss model applied. Figure 5 also indicates that the heat losses slow down the system transient response in the HTDF.

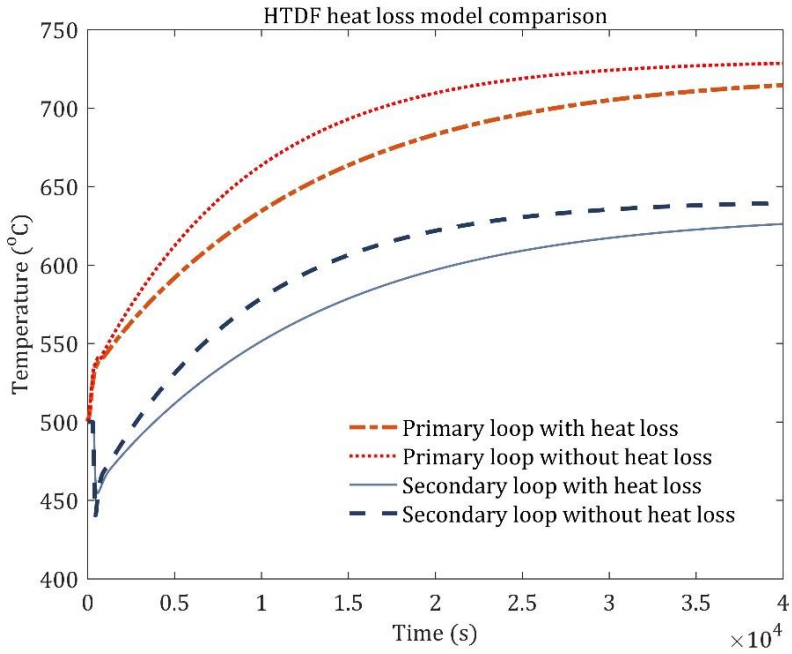

Figure 5. Salt temperature comparisons in the HTDF with and without the heat loss model applied.

4. Results and Discussions

A benchmark study was performed to assist developing a competent DRACS thermal-hydraulic model in RELAP5. The LTDF RELAP5 model includes the heat loss model and utilizes the heat transfer correlations implemented for the heat exchangers. Two types of scenarios were considered in the benchmark study, namely, the DRACS startup and primary pump trip. In addition to the LTDF model benchmark with available experimental data, the

HTDF model was also developed to provide DRACS simulation results during the two transients.

4.1. LTDF Startup Scenario

The startup scenario in the LTDF demonstrates the establishment of natural circulation/convection after the heat up of the primary water while the coolants in the three loops are all stagnant initially. One of the branches in the primary loop where the primary pump is located. The pump side of primary loop is closed by a valve, so the primary water only can flow through the DHX branch. When the DRACS startup scenario is initiated, a constant heating power of 2 kW is provided to the system by the electric heaters, based on 1% of the core decay power (200 kW) in the prototypic reactor design. The benchmark of the RELAP5 simulation results with the LTDF experimental data for the DRACS startup baseline case is discussed first.

Figure 6 to Figure 9 show the benchmark results of the fluid temperatures and mass flow rates in the three loops, with a time scale of 0 to 30,000 s. The temperature transient responses from both the experiment and simulation indicate that the system reaches a quasi-steady state at approximately 16,000 s from the event initiation when the temperature difference between inlet and outlet of DHX and NDHX are close to a constant. Figure 6 shows the water inlet and outlet temperatures on the DHX shell side in the primary loop (i.e., the primary water in DHX in on the shell side and DRACS water in DHX and NDHX is on the tube side.). At 30,000 s, the water inlet and outlet temperatures on the DHX shell side obtained from the RELAP5 simulation are approximately 6 °C lower than those in the experimental data, which represents an error of approximately 7%. The water inlet and outlet temperatures on the DHX tube side

(i.e., the DRACS loop) are shown in Figure 7. Compared to the experimental results, the RELAP5 simulation over-predicts the DHX tube-side temperatures by approximately 4 °C. Figure 8 shows the NDHX air-side inlet and outlet temperatures from both the experiment and RELAP5 simulation. The air-side inlet temperature is given by the actual values measured in the experiment (Note the relatively large air temperature variation, over 6 ^{o}C, during the 30,000 s of the experiment time). The overall fluid temperature responses in the three loops from the RELAP5 simulation results exhibit reasonably good agreement with the experimental data during the DRACS startup transient. It should be noted that the relatively large discrepancies in the water temperatures between the experimental data and RELAP5 results shown in Figures 6 and 7 are believed to be due to the heat transfer correlations used for the DHX and NDHX heat exchangers. From Figure 9, it is clear that natural circulation flows are gradually established during the transient. As shown in the experimental data, the air mass flow rate remains oscillatory throughout the experiment duration. This is primarily because the air inlet chimney points to a fix direction and thus is heavily affected by the natural wind (direction and wind speed).

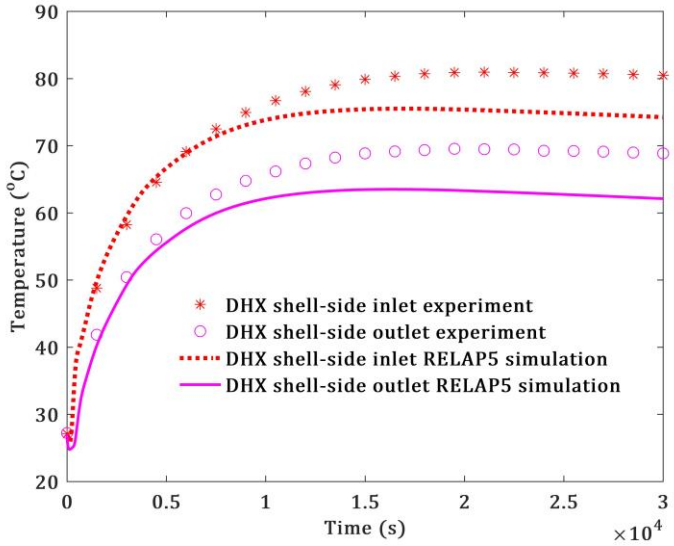

Figure 6. LTDF benchmark results of the DHX shell-side (primary loop) water inlet and outlet temperatures during DRACS startup transient.

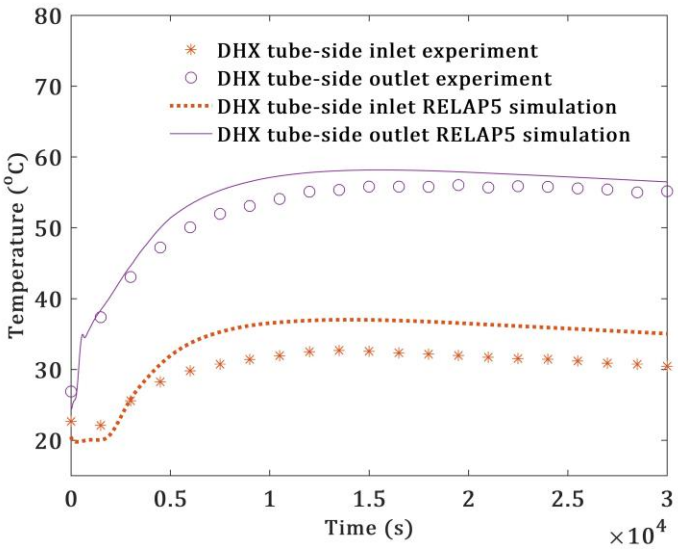

Figure 7. LTDF benchmark results of the DHX tube-side (DRACS loop) water inlet and outlet temperatures during DRACS startup transient.

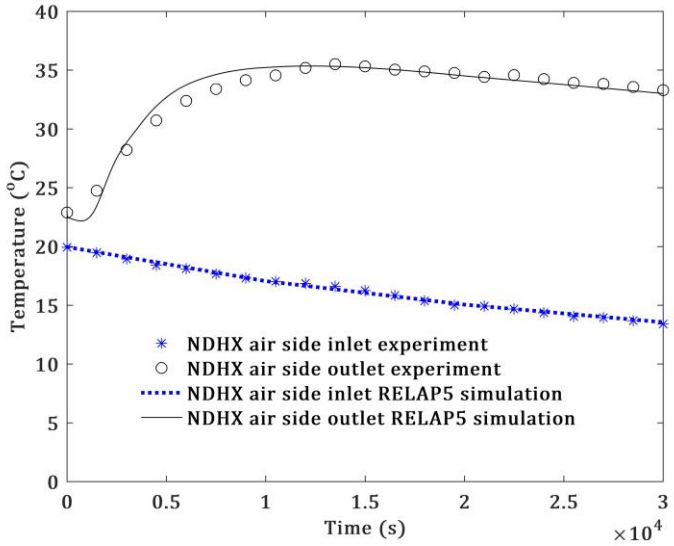

Figure 8. LTDF benchmark results of the air inlet and outlet temperatures during DRACS startup transient.

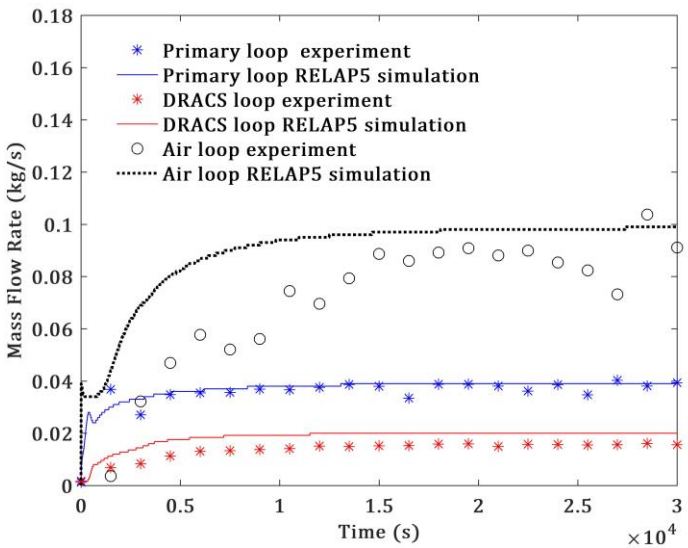

Figure 9. LTDF benchmark results of the fluid mass flow rates in the three loops during DRACS startup transient.

4.2. LTDF Pump Trip Scenario

The primary pump trip scenario represents the event of loss of forced flow (LOFF) in FHRs. The DRACS thermal performance under natural circulation condition is studied in this scenario. For the initial condition, the primary pump provides a constant water mass flow rate of 1.75 kg/s in the primary loop with 0.04 and 1.71 kg/s in the DHX-side branch and the simulated core branch, respectively. A constant heating power of 2 kW is given in the simulated core before and after pump trip. At time 0 s, the primary pump and reach fully stop at 20 s. Figure 10 shows that when the primary pump trip is initiated, the primary loop loses its driving force and that the flow in the primary loop (in the DHX-side branch) reverses due to the buoyancy and a much smaller flow resistance in the fluidic diode's forward (downward) direction. After the flow reversal, a natural circulation flow in the primary loop is established.

Figures 11-13 provide the benchmark results of the temperature transient responses in the three loops. Similar to the DRACS startup scenario, the NDHX air-side inlet temperature is obtained from the experimental data and is used as a boundary condition in the RELAP5 calculation. The air inlet temperature decreases with time, which causes the fluid temperatures in the three loops to decrease as well. In Figure 11, the DHX shell-side inlet temperature peak is resulted from the sudden flow decrease in the primary loop after the loss of driving force from the primary pump. In addition, the RELAP5 simulation results show faster temperature decreases in both the DHX shell-side inlet and outlet temperatures as compared to the experiments. This is primarily due to the heat losses and the discrepancy of thermal inertia in the structures between the LTDF model and experiment. From the benchmark results for the primary pump trip scenario, we can conclude that reasonably good agreement between the experimental data

and RELAP5 simulation results are obtained and that the DRACS system provides a sufficient heat removal capability.

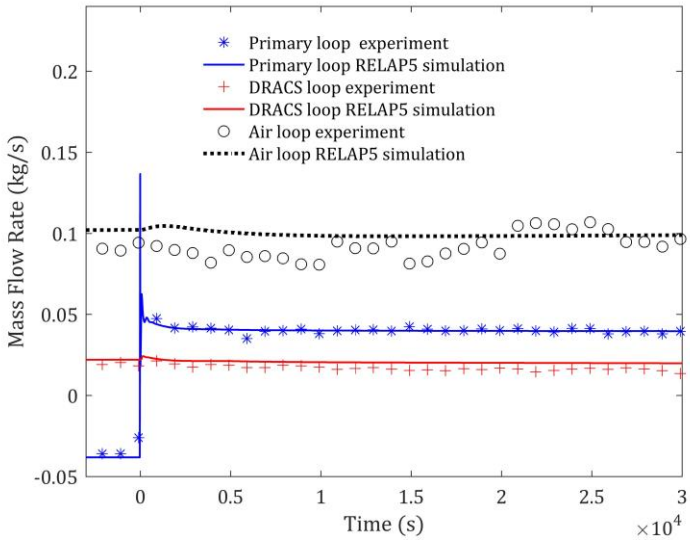

Figure 10. LTDF benchmark results of the mass flow rates in the three loops during the primary pump trip scenario.

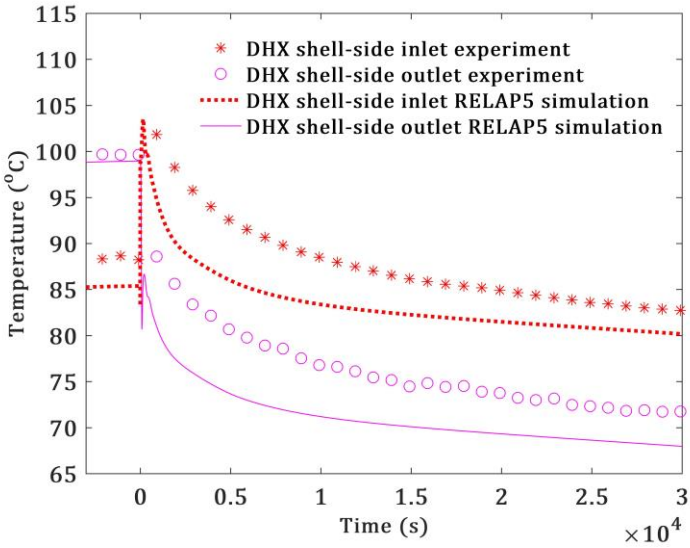

Figure 11. LTDF benchmark results of the DHX shell-side (primary loop) water inlet and outlet temperatures during the primary pump trip scenario.

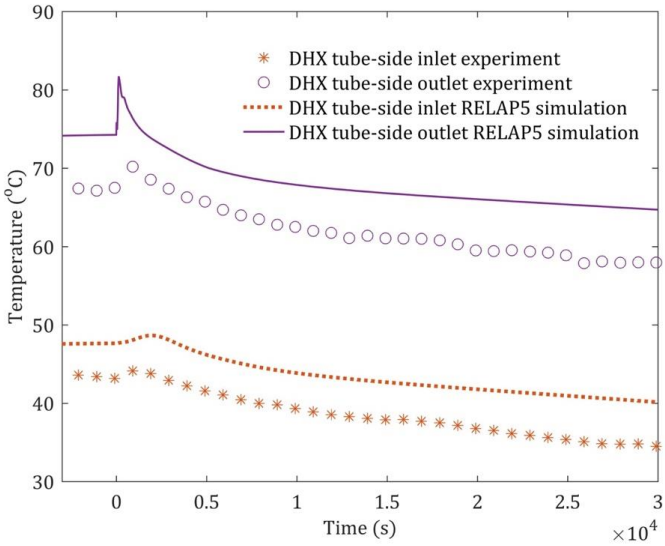

Figure 12. LTDF benchmark results of the DHX tube-side (DRACS loop) water inlet and outlet temperatures during the primary pump trip scenario.

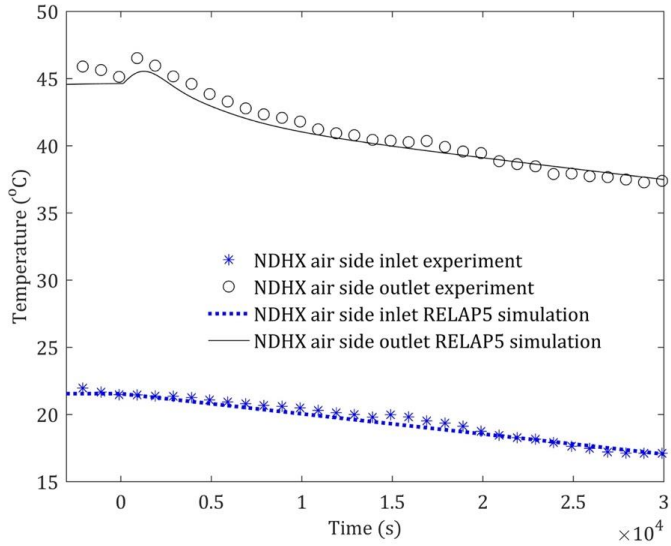

Figure 13. LTDF benchmark results of the air inlet and outlet temperatures during the primary pump trip scenario.

Figures 10-13 show the results for the primary pump trip scenario where a constant 2 kW power from the core is provided before and throughout the transient. In a different test, the decay power curve as a function of the reactor cooling time is considered. Figure 14 gives the decay power curve, which is the decay curve for light water reactors (LWRs) (El-Wakil et al., 1971). Because of the maximum power limitation of the three electric heaters in the LTDF, a constant maximum heating power of approximately 4,983 W is therefore provided before 1,564 s. The total amount of decay energy deposit in the DRACS primary loop following the modified decay curve is however the same as that following the original LWR decay curve from 0 to 1,564s. After 1,564 s, the decay power applied by the electric heaters in the LTDF follows the LWR decay curve. Figure 15 shows a comparison of the DHX shell-side inlet and outlet temperatures between the experimental data and RELAP5 simulation for the second primary pump trip scenario. The simulation results show faster transient responses, but the overall trends are similar with experimental data.

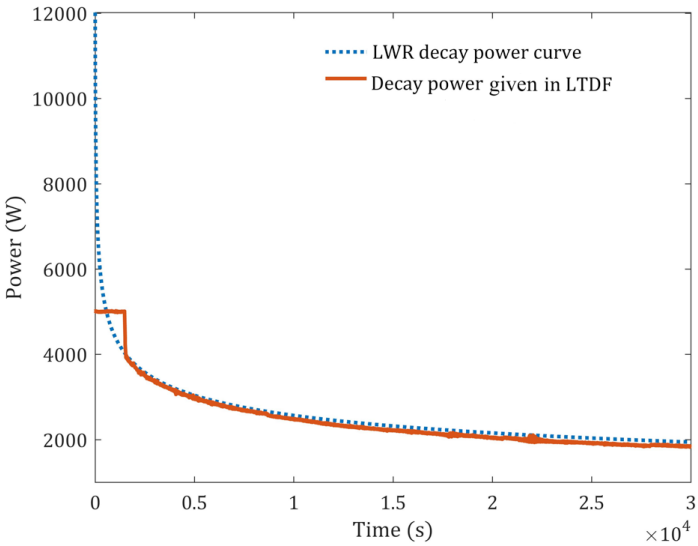

Figure 14. Adopted decay power curve in the LTDF for the second primary pump trip scenario

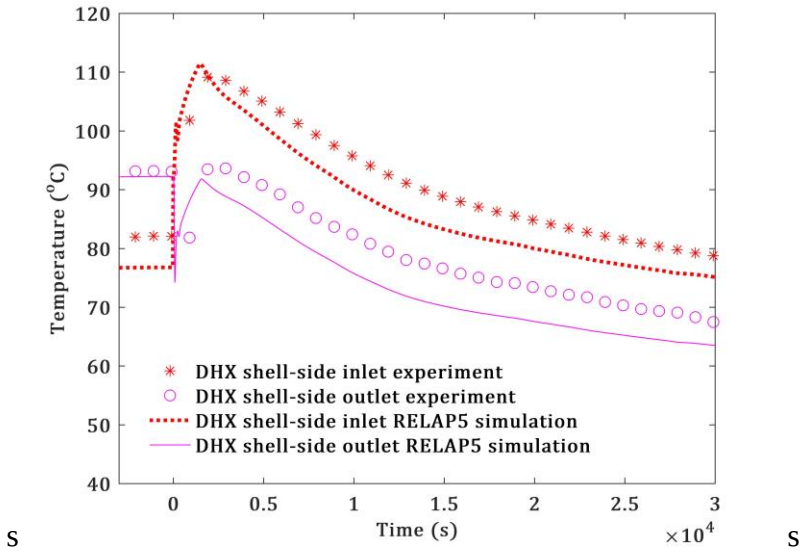

s s

Figure 15. LTDF benchmark results of the DHX shell-side (primary loop) water inlet and outlet temperatures during the second primary pump trip scenario.

4.3. Simulation of the HTDF

As mentioned earlier, experiments in the HTDF have not been performed yet. In the HTDF RELAP5 model, the initial salt temperatures in the primary and DRACS loops are set at 500 °C and the air inlet temperature is assumed as a constant of 40 °C. For the DRACS startup scenario in the HTDF, all fluids are set to be stagnant initially. The simulated core provides a 10-kW constant power when the transient is initiated. The DRACS startup simulation results in the HTDF are shown in Figure 16. The primary salt (DHX shell side) and DRACS coolant (NDHX tube side) temperatures can reach above 700 and 650 °C, respectively. Before 1,000 s into the transient, the NDHX tube-side KF-ZrF_4 temperature decreases rapidly due to the large temperature difference between the DRACS loop and the ambient air, leading to a rapid cooling of the DRACS salt, as shown in Figure 16. To prevent the molten salt from freezing by rapid cooling, a sufficient temperature margin above the salt melting point should be provided to the molten DRACS salt during the DRACS startup scenario.

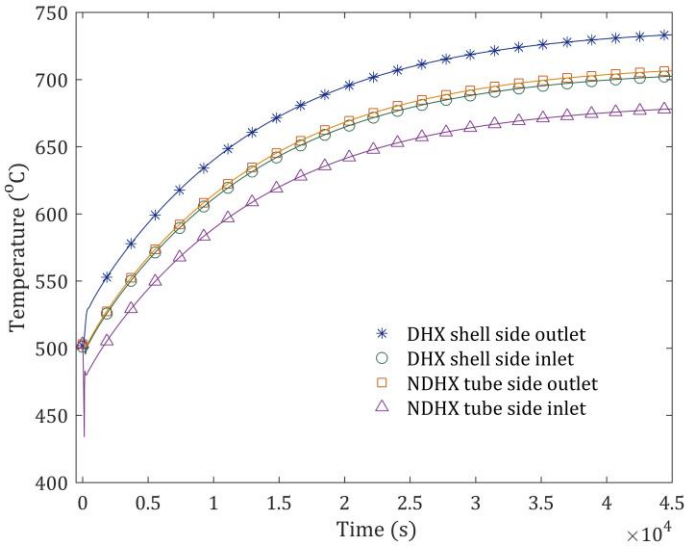

Figure 16. RELAP5 simulation results of DHX shell side (primary loop) and NDHX tube side (DRACS loop) temperatures in HTDF during the DRACS startup scenario.

In addition to KF-ZrF_4, FLiNaK is another coolant salt candidate for the DRACS loop in the HTDF. However, the freezing point of FLiNaK is relatively high as compared to KF-ZrF_4 and therefore, FLiNaK could be overcooled. To prevent FLiNaK from freezing, Figure 17 demonstrates that when the air loop is closed initially and then opened at 1,000 s, such an air chimney operation can effectively mitigate the phenomenon of rapid salt temperature drop in the NDHX tube side outlet (DRACS loop cold leg). In addition, the air loop is also heated up in the closed chimney chamber and the air temperature rises above 500 °C. After the air chimney is opened, the air outlet temperature immediately decreases and reaches a stable value.

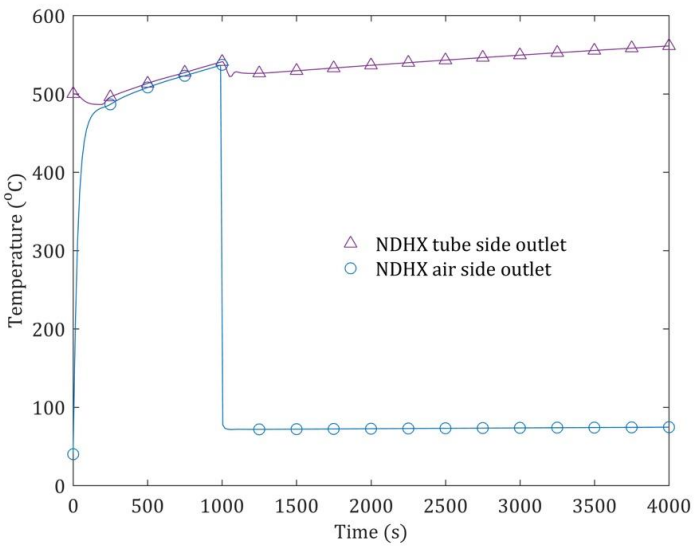

Figure 17. DRACS salt and air temperatures from the RELAP5 HTDF simulation during the DRACS startup scenario.

The HTDF model is also used to simulate the primary pump trip scenario. In the simulation, a constant heating power of 9 kW is provided initially till a steady state is reached before initiating the transient. After the primary pump is tripped, the core heating power in the HTDF model increases to 10 kW. In the pump trip scenario, there is no rapid cooling mechanism and therefore, salt freezing problem is insignificant. In this simulation, the pump is assumed to have

a complete stop at 20 s after the pump trip event is initiated. It should be noted that there is no design information available in the literature regarding the primary salt coolant pump behavior after shutdown. Therefore, pump coast down behavior should be further investigated in future experiments since the salt flow will affect the salt peak temperatures as well as the thermal stresses in key components, such as the heat exchangers and piping. The salt peak temperature at the DHX shell-side (primary salt) outlet reaches 740 °C, which does not appear to be a significant temperature increase as compared to the primary salt peak temperature during reactor normal operation. This however may represent a challenge to structural materials in FHRs as the current most promising structural material, Hastelloy N is codified to a maximum temperature of 704 ^{o}C for nuclear applications by the ASME code. The transient response confirms that the scaled-down DRACS provides a stable and sufficient heat removal capability during the primary pump trip scenario. When performing the RELAP5 model validation against the HTDF experimental data once available, we should note that the uncertainties in the implemented salt thermophysical properties will affect the degree of agreement between the code results and experimental data.

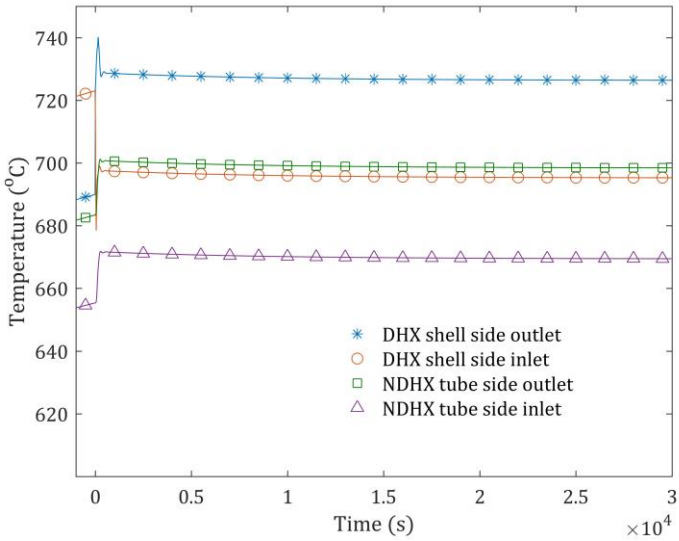

Figure 18. RELAP5 simulation results of DHX shell side (primary loop) and NDHX tube side (DRACS loop) temperatures in HTDF during primary pump trip

5. Conclusions

The primary objectives of this study are to investigate the thermal performance of the DRACS during transient scenarios and to perform a system-level analysis code validation using the experimental data. The simulation results by RELAP5/SCDAPSIM/MOD 4.0 are compared with the LTDF experimental data for two transients, namely, the DRACS startup and primary pump trip transients. The pipe structures, flanges, and thermal insulations are included in the LTDF RELAP5 model for heat loss analysis. The simulation shows that approximately 7% of heat addition to the DRACS system in the LTDF is lost to the ambient environment. Both the experimental and RELAP5 simulation results indicate that although the temperature responses of the entire DRACS system can be affected by the daily variation of the ambient air temperature, the overall DRACS thermal performance can still be clearly observed and its functionality be confirmed.

The thermodynamic and transport properties of FLiNaK and KF-ZrF_4 have been successfully implemented into the RELAP5/SCDAPSIM/MOD 4.0 code, which was used to model the thermal performance and transient response of the HTDF. The heat loss model is also applied in the HTDF model, and with a better and thicker thermal insulation used in the HTDF, about 3% of the total heat added to the DRACS system would be lost to the environment, which leads to an approximately 10°C temperature decrease in the primary coolant salt. The RELAP5 simulation results of the HTDF show similar trends observed in the LTDF for the two transients, i.e., the DRACS startup and primary pump trip. In the HTDF startup scenario, the rapidly decreasing temperature in the cold leg of the DRACS loop may cause freezing of the DRACS salt, which could be prevented by controlling the air flow rate or providing additional trace heating. The benchmark study of the HTDF RELAP5 model will be performed once the HTDF experimental data become available.

Acknowledgments

This research was performed using funding received from the US Department of Energy (DOE) Office of Nuclear Energy's Nuclear Energy University Program (NEUP). The authors appreciate the financial from the DOE NEUP office and technical support from the technical point of contact Dr. David Holcomb of the Oak Ridge National Laboratory.

References

Allison, C.M., Wagner, R.J., Hohorst, J.K., Perez-Ferragut, M., Martinez-Quiroga, V., Freixa, J., de les Valls, E.M., Fu, Z., Lin, H.C. and Lou, M., 2015. The development of

RELAP/SCDAPSIM/MOD4. 0 for advanced fluid systems design analysis. In: Proc. of NUTHOS-11, Gyeongju, Korea, October 9-13.

Anderson, N.A. and Sabharwall, P., 2012. Molten salt mixture properties ($KF-ZrF_4$ and $KCl-MgCl_2$) for use in RELAP5-3D for high-temperature reactor application. Nuclear Technology, 178, pp. 335-340.

Bardet, P., Blandford, E., Fratoni, M., Niquille, A., Greenspan, E., Peterson, P.F., 2008. Design, analysis and development of the modular PB-AHTR. In: Proc. of ICAPP'08, Anaheim, CA, June 8–12.

Chen, M., Kim, I.H., Sun, X., Christensen, R., Utgikar, V. and Sabharwall, P., 2015. Transient analysis of an FHR coupled to a helium brayton power cycle. Progress in Nuclear Energy, 83, 283-293.

Chen, M., Sun, X., Christensen, R., Shi, S., Skavdahl, I., Utgikar, V. and Sabharwall, P., 2016. Design and testing of helicallycoiled fluted tube heat exchangers for FHR applications. In: 11th International Topical Meeting on Nuclear Reactor Thermal Hydraulics. Gyeongju, South Korea, Oct 9-13.

Davis, C., 2005. Implementation of molten salt properties into RELAP5-3D/ATHENA. INEEL/EXT-05-02658, Idaho National Laboratory, Idaho Falls, ID.

El-Wakil, M. M., 1971. Nuclear Heat Transport. International Textbook Co., Scranton, PA

Forsberg, C.W., 2005. The Advanced High-Temperature Reactor: high-temperature fuel, liquid salt coolant, and liquid-metal-reactor plant. Prog. Nucl. Energy, 47(1–4), 32–43.

Forsberg, C.W., Pickard, P., and Peterson, P.F., 2003. Molten-salt-cooled Advanced High Temperature Reactor for production of hydrogen and electricity. Nucl. Technol., 144, 289–302.

Holcomb, D.E., Cetiner, S.M., Flanagan, G.F., Peretz, F.J., Yoder, G.L., 2009. An analysis of testing requirements for fluoride salt-cooled high temperature reactor components. ORNL/TM-2009/297, Oak Ridge National Laboratory, Oak Ridge, TN.

Lin, H.C., Lv, Q., Shi, S., Sun, X., Christensen, R.N., Blue, T.E., Sabharwall, P., 2016. RELAP5 Model Validation and Benchmark for DRACS Thermal Performance. In: Proc. of ICAPP'16, San Francisco, CA, US, April 17-20.

Lv, Q., Chen, M., Sun, X., Christensen, R., Blue, T., Yoder, G., Wilson, D. and Sabharwall, P., 2013. Design of fluidic diode for a high-temperature DRACS test facility. In: 2013 21st International Conference on Nuclear Engineering, Chengdu, China, July 29-Aug 2.

Lv, Q., Lin, H.C., Kim, I.H., Sun, X., Christensen, R.N., Blue, T.E., Yoder, G.L., Wilson, D.F., Sabharwall, P., 2015. DRACS thermal performance evaluation for FHR. Annuals of Nuclear Energy, 77, 115-128.

Lv, Q., Lin, H.C., Shi, S., Sun, X., Christensen, R.N., Blue, T.E., Yoder, G.L., Wilson, D.F., Sabharwall, P., 2016. Experimental Study of DRACS Steady-State and Transient Performance. In: Proc. of ICAPP'16, San Francisco, CA, April 17-20.

Lv, Q., Lin, H.C., Sun, X., Christensen, R., Blue, T., Yoder, G., Wilson, D., Sabharwall, P., 2015. Experimental study of DRACS thermal performance in a low-temperature test facility. In: Proc. of NURETH-16, Chicago, US, Aug 30-Sep. 4.

Roglans, J., Ragland, W., and Hill, D., 1993. A PRA case study for extended long term decay heat removal for shutdown risk assessment. In: American Nuclear Society International Topical Meeting on Probabilistic Safety Assessment, American Nuclear Society, Clearwater Beach, FL.

Williams, D., 2006. Assessment of candidate molten salt coolants for the NGNP/NHI heat transfer loop. ORNL/TM-2006/69, Oak Ridge National Laboratory, Oak Ridge, TN.

Wang, D., Yoder, G.L., Pointer, D.W. and Holcomb, D.E., 2015. Thermal hydraulics analysis of the Advanced High Temperature Reactor. Nuclear Engineering and Design, 294, 73-85.

Zhang, H., Zhao, H., Mousseau, V., and Szilard, R., 2009. Design considerations for economically competitive sodium cooled fast reactors. In: Proc. of ICAPP'09, Tokyo, Japan, May 10–14.

Zkauskas, A., 1987. Heat transfer from tubes in cross flow. Advances in Heat Transfer, 18, 87-159.

Zukauskas, A. and Ulinskas, R., 1988. Heat transfer in tube banks in cross flow. Taylor & Francis.